Macondo oil in northern Gulf of Mexico waters – Part 2: Dispersant-accelerated PAH dissolution in the *Deepwater Horizon* plume

William B. Driskell [a] and James R. Payne [b]

[a] 6536 20th Ave NE, Seattle, WA 98115
bdriskell@comcast.net

[b] Payne Environmental Consultants, Inc., 1651 Linda Sue Ln, Encinitas, CA 92024
jrpayne@sbcglobal.net

Abstract

During the *Deepwater Horizon* blowout, unprecedented volumes of dispersant were applied both on the surface and at depth. Application at depth was intended to disperse the oil into smaller microdroplets that would increase biodegradation and also reduce the volumes buoyantly rising to the surface, thereby reducing surface exposures, recovery efforts, and potential stranding. In forensically examining 5,300 offshore water samples for the Natural Resource Damage Assessment (NRDA) effort, profiles of deep-plume oil droplets (from filtered water samples) were compared with those also containing dispersant indicators to reveal a previously hypothesized but undocumented, accelerated dissolution of the polycyclic aromatic hydrocarbons (PAH) in the plume samples. We interpret these data in a fate-and-transport context and conclude that dispersant applications were functionally effective at depth.

Keywords

Dispersant effect; PAH dissolution; aliphatic hydrocarbons; oil droplet; *Deepwater Horizon;* microbial degradation.

Introduction

During the *Deepwater Horizon* (DWH) blowout, an unprecedented 1.07 million gallons of dispersants were applied to the surface from aircraft and boats (~88% as the Corexit 9500 formulation and ~12% as Corexit 9527) and an additional 771,000 gallons of Corexit 9500 were injected subsurface into the oil plume directly at the wellhead (1,528m depth) (BP, 2014). When dispersants are effectively applied to surface slicks, the resulting dispersed oil weathers quicker and is more readily entrained by turbulence into near-surface waters where it is less susceptible to being driven into intertidal habitats (NRC, 2005; Katz, 2009). At depth, dispersant remediation was intended to enhance breakup of oil into smaller micro-droplets that would subsequently rise slower (if at all) through the water column, weather quicker, and form fewer surface slicks (CRRC, 2010). Keeping the oil submerged would also reduce response-personnel and natural-resource exposure to volatile aromatic and aliphatic components (Ryerson et al., 2011).

Chemically dispersing oil is physically accomplished by the surfactant's molecular oleophilic end attaching to the oil's surface in sufficient concentration to reduce the oil's local surface tension and thereby create a micro-eruption that subsequently re-forms into smaller micro-droplets (Katz, 2009; Gopalan and Katz, 2010). At the sub-millimeter scale, Gopalan and Katz demonstrated how a crude oil droplet mixed with dispersant shears into formations of localized regions having low surface tension that produce very long, µm-sized oil threads trailing behind the droplets (aka "tip streaming") (Figure 1 and Figure 2). The shearing energy may be caused by interaction with micro-scale turbulence from a

simple buoyant rise (Figure 2) or from mega-scale events such as splashing rainfall or breaking waves (Murphy et al., 2015; Katz et al., 2013; Li et al., 2013; Nagamine, 2104; Li et al., 2016). Eventual breakup of these threads into µm-sized droplets follows, presumably occurring from a reduced dispersant-to-oil ratio (DOR) as the surface area increases and/or the water-soluble dispersant diffuses into the surrounding fluid. Eventually, the restored surface tension reforms the smaller droplet(s).

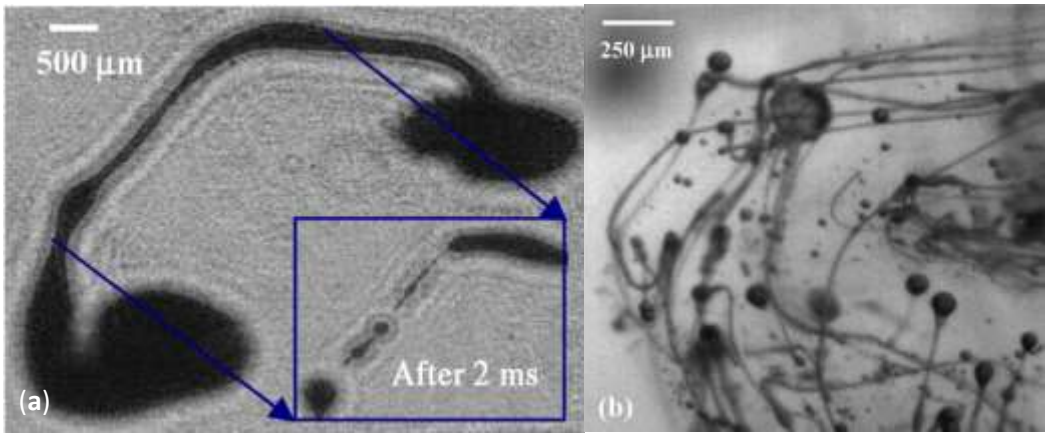

Figure 1. Images showing a) turbulent stretching of a crude oil droplet for a volumetric dispersant-to-oil ratio (DOR) of 1:20, with inset showing the capillary breakup of a section 2 ms later and b) droplets with long threads trailing behind them, which are produced when a water jet impinges on a surface layer of oil mixed with dispersant (DOR 1:15)). (Images used with permission from Balaji Gopalan and Joseph Katz, Johns Hopkins University).

Figure 2.Dispersed oil droplet shedding microdroplets while rising. (Image used with permission from David Murphy and Cheng Li, Johns Hopkins University).

Corexit dispersants used during the DWH event were lab and field-tested under NOAA Special Monitoring of Applied Response Technologies (SMART) protocols to empirically demonstrate their utility (Bejarano et al., 2013). One effect hypothesized from lab simulations and modeling but not previously proven was that dispersant-treated oil droplets, because of their smaller droplet size and resulting very high surface-area-to-volume ratio, could lose their water-soluble, lower-molecular-weight PAH more quickly than non-dispersed oil (NRC, 2005), i.e., they would weather quicker–an obviously important factor in evaluating dispersed oil's dissolved-phase bioavailability/toxicity and in modeling both non-dispersed and dispersant-treated oil's fate and behavior. From early DWH field data, Payne and Beegle-

Krause (2011) demonstrated the co-occurrence of water-soluble dispersant components and dissolved-phase oil PAH in the sub-surface plume but could not determine from just chemistry data whether the subsurface injection of the dispersants actually enhanced the breakup of the oil into smaller droplet sizes. To confirm this process, it was necessary to find dispersant components still present in the water's filtered-oil phase, i.e., still attached to the droplets.

Also, prior to the DWH event, it had not been documented that the active surfactant component, dioctyl sodium sulfosuccinate (DOSS), and the glycol-ether carrier solvent would be conserved (Gray et al., 2011, 2014; White et al., 2014). In 2011, Kujawinski et al. first reported evidence of DWH dispersants, within the depth range of the deep plume (~1,200 m) and with confirming fluorescent indications, persisting up to 300 km from the well and 64 days after the wellhead dispersant applications ceased. The 5,300 offshore NRDA samples we evaluated also confirmed that dispersant indicators were associated with both particulate (filtered) oil and the dissolved phase at the entrapped plume depth (Payne and Driskell, 2018, Part 1 of this series). Furthermore, fluorescence and dissolved oxygen features suggested an extant plume with conserved dispersant-derived components up to 412 km southwest from the wellhead (albeit without confirming a relevant GC/MS-detectible PAH profile) (Payne and Driskell, 2015a; Payne and Driskell, 2018). By the mid-event sampling in 2010, various particle imaging systems also confirmed the diminished droplets created by dispersants at depth (Davis and Loomis, 2014; Payne and Driskell, 2015b; French-McCay et al., 2015, 2018; Li, et al., 2015, 2016). For this paper, we present the immediate effects of dispersant on the DWH oil's PAH components.

Methods

During the DWH event, offshore water-column samples for the NRDA were primarily collected using Niskin or GoFlo bottles mounted on instrumented multi-bottle, rosette frames or using a submersible remotely-operated vehicle (ROV) (Payne and Driskell, 2015b; Payne and Driskell, 2016, 2018). Samples reviewed in this study were collected in 2010 and primarily within 20 km of the wellhead. Knowing the utility of distinguishing dissolved- from particulate-phase oil when interpreting oil fate and transport processes, a concerted effort was made on various NRDA cruises to obtain phase-discriminated sub-samples using portable field-filtering equipment (Payne et al., 1999, Payne and Driskell, 2018). Thus, from offshore cruises, four water-sample matrices were reported: volatile organics (40 mL), whole water (1 L), and from the filter-processed samples, the complimentary paired dissolved-phase (~3.5 L) and particulate/oil-phase (filter) matrices.

In the laboratory, samples were spiked with appropriate deuterated surrogates and triple-extracted with dichloromethane (DCM) but, as water samples, without silica-gel cleanup. Extracts were spiked with internal standards and analytic quantifications performed in accordance with the NOAA (2014) DWH Analytical Quality Assurance Plan (AQAP) for:

- Total Extractable Material (TEM) and Saturated Hydrocarbons (SHC)—a modified EPA Method 8015B was used to determine the summed concentration of TEM (C_9-C_{44}) and individual concentrations of the saturated n-alkanes (C_9-C_{40}) and selected (C_{15}-C_{20}) acyclic isoprenoids (e.g., pristane and phytane) that constituted the SHC. This method also provided a high-resolution gas chromatography-flame ionization detector (GC/FID) fingerprint of the samples.
- PAH, Alkylated PAH, and Petroleum Biomarkers—semi-volatile compounds were analyzed using selected ion monitoring gas chromatography/mass spectrometry (SIM GC/MS) via a modified

EPA Method 8270. This analysis provided the concentrations of 1) approximately 80 PAH, alkylated PAH homologues, individual PAH isomers, and sulfur-containing aromatics and 2) approximately 50 tricyclic and pentacyclic triterpanes, regular and rearranged steranes, and triaromatic steroids.

- Volatile hydrocarbon samples from whole water (non-filtered) samples were analyzed for benzene, toluene, ethylbenzene and xylenes (BTEX) and other constituents by a purge-and-trap protocol under a modified EPA method 8260.

For forensic purposes, concentrations were reported as non-surrogate-corrected values on a per-volume basis in ng/L (ppt) for PAH and biomarkers, and as µg/L (ppb) for SHC and BTEX.

In NRDA forensic reviews, the presence of dispersant was indicated by detection of DOSS or other dispersant indicators. DOSS, which comprises 10-30% by weight of the DWH Corexit formulations, is too large and too polar for conventional gas chromatography/mass spectrometry (GC/MS). At ALS (Kelso, WA) and various academic and agency labs, DOSS was analyzed in water samples using a newly developed, high-performance liquid chromatography/mass spectrometry (LC/MS) method (Gray et al., 2011, 2014; and Kujawinski et al., 2011). From the primary NRDA forensic laboratory, Alpha Analytical Laboratory (Mansfield, MA), just the confirmation of dispersants was considered sufficient for forensic needs and thus, standard selected-ion-monitoring GC/MS (modified Method 8270) without further fractionation or cleanup was used to semi-quantify water-borne, Corexit-derived components. Dispersant indicators reported by Alpha included:

- di(propyleneglycol)-n-butyl ethers), designated as "GE" for glycol ethers, and C_9-C_{14} petroleum distillates (commercially, Nopar 13), the major solvents in Corexit 9500
- 2-butoxyethanol, a major solvent in Corexit 9527 designated herein as "2BE" but also a filter contaminant in field-filtered samples, and
- bis(2-ethylhexyl)fumarate, a DOSS-derived, GC injection-port-heat-breakdown product associated with both Corexit 9527 and 9500 (Stout, 2015).

Fingerprinting

Dispersant-mediated weathering effects to the oil's PAH profile were markedly different from normal oil-seawater dissolution patterns (Figure 3). Because the effects were only evident as losses in particulate-phase profiles, the sample set was limited to MC252-confirmed samples containing a particulate DWH profile (n = 493 of 4,189). Note that Supplemental Information for Part 1 of this series (Payne and Driskell, 2018) presented a method to forensically confirm a sample profile's source and parse out particulate and dissolved portions. From this fingerprinting task, particulate samples containing high levels of the glycol ethers dispersant component displayed anomalous weathering profiles, which eventually lead to identifying unique properties of dispersant-mediated profiles (discussed in more detail in Payne and Driskell, 2015d). Seven characteristics distinguished a dispersant-mediated profile:

- Presence of dispersant indicators (often at very high concentrations); DOSS, glycol ethers (GE), or 2-butoxyethanol (2BE). The 2BE was also a confounding contaminant suspected arising from the filters used in filtered samples. For unknown reasons, a fourth reported component, bis(2-ethylhexyl) fumerate, was not a reliable indicator. Note that some early samples were not analyzed for dispersants (prior to 25 July 2010 at Alpha Laboratory).

- A very weathered PAH profile with accelerated loss of light alkylated ends up through dibenzothiophenes.
- A very distinctive water-washed chrysene pattern with C0<C1<C2<C3<C4.
- Significant SHC often present that, based on n-C_{17}/pristane and n-C_{18}/phytane ratios, was not completely microbially degraded.
- Alkylated dibenzothiophene/phenanthrene (D/P) ratios on atypical low-trend path in double-ratio plots (D2/P2 vs D3/P3).
- Decalins, the saturated bicyclic "pseudo-PAH" dominant in Corexit, may be present and sometimes high, and
- In dissolved-phase samples (the associated complements of filtered particulate-phase samples), fluorenes were often in excess relative to phenanthrenes.

Samples displaying some or most of these characteristics would be considered "dispersant-mediated" or "dispersed." The presence of the dispersant indicator, GE, was not a requisite because the particulate and dissolved phases of the source oil may have disassociated into separate water parcels. Also, GE data were not available for part of the dataset as GE was not quantified in early samples. "Non-dispersed" samples were missing the relevant dispersed profile characteristics.

Results

Dispersant Effects

From the near-bottom jetted oil and gas of the DWH blowout (MC252 oil, from Macondo Formation, lease block 252), an entrained plume formed at ~1,000-1,400 m depth comprising small oil droplets (6-300 µm, Li et al., 2015, 2016) trapped by their near-neutral buoyancy (Socolofsky et al., 2011; Spaulding et al., 2015). Eventually advected from the wellhead area, the plume was carried by deep currents with net movement to the southwest. Unlike the larger, more buoyant droplets (>300 µm) that rose rapidly and eventually reached the surface, the only weathering processes affecting the small oil droplets were dissolution and microbial degradation, i.e., at the entrapment depth, there were no evaporative or photo-oxidation losses. These more controlled circumstances at depth created an opportunity to evaluate the effects of the dispersants injected directly into the blowout. These dispersants were hypothesized to affect a more rapid dissolution process and perhaps microbial degradation but the effects were more unexpected and dramatic. In the observed hydrocarbon profiles (presented below), PAH dissolution was initially accelerated and relative SHC degradation delayed.

From fundamental chemistry, hydrocarbon water solubility is generally related to the inverse of molecular weight, e.g., two-ringed aromatic naphthalenes are more soluble than the four-ringed chrysenes, which are nearly insoluble. In addition, within each PAH group, dissolution losses inversely correlate with the degree of alkylation, i.e., components within each group's alkylated "hump" distribution pattern (Figure 3 upper right) are less soluble with increasing carbon-number and molecular weight, as expressed by their octanol/water partition coefficient (K_{OW}). In the DWH particulate-phase samples lacking dispersant indicators, these predictable weathering patterns were observed and served as the general basis for oil-spill forensics analysis and modeling (Payne and Driskell 2015c and references

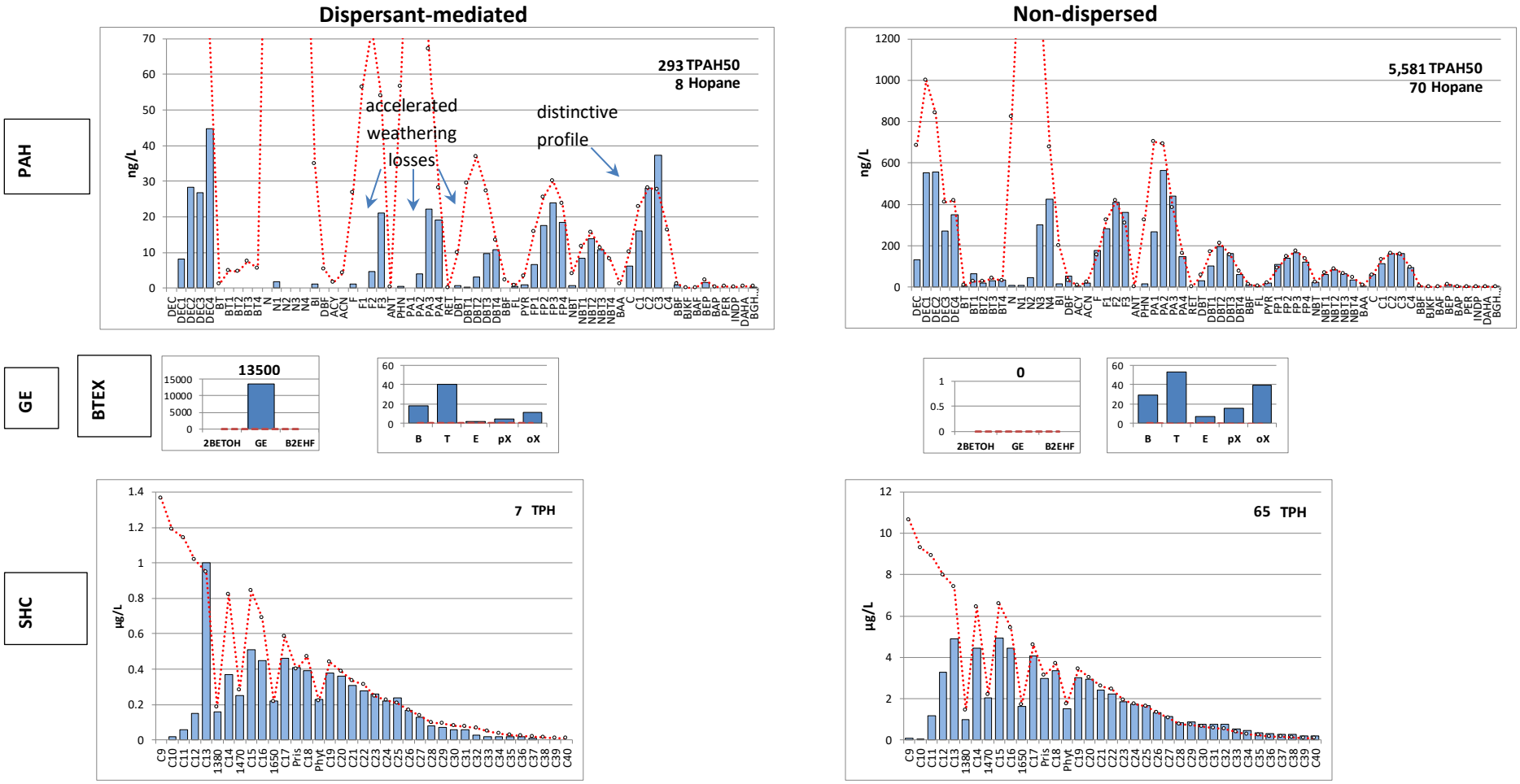

Figure 3. Dispersant effects on oil profiles as shown by typical deep-plume, dispersant-mediated, whole-water sample (left panels) whereby a heavily weathered PAH profile (top left, with dotted red line representing fresh MC252 reference scaled to C2-chrysene) shows accelerated weathering of naphthalenes through C-3 dibenzothiophenes, a distinctive chrysene pattern (right PAH group), high levels of the dispersant indicator, glycol ethers (GE, center left plots), high concentrations of BTEX (center right plots), and unexpectedly fresh, only partially degraded SHC (lower left plot) relative to the extent of PAH weathering. Compare with normal, non-dispersant-mediated, weathered sample in right plots. Hopane was measured but biomarkers were not acquired in these early samples.

therein; Payne and Driskell, 2018, Figure 3 upper right). In contrast, samples containing dispersant indicators (hereafter, "dispersant-mediated samples") showed additional weathering from accelerated abiotic dissolution of the lower- and intermediate-molecular-weight PAH (Figure 3 upper left).

For example, comparing the differences in loss of the alkylated C2- and C3-phenanthrene/anthracenes (PA2 and PA3, normalized to each sample's C2-chrysene) between chemically-dispersed and non-dispersed samples shows that the relative PA2 and PA3 concentrations are significantly different between the two treatment groups (Figure 4). In contrast, no significant difference is evident in distributions of the mostly insoluble C2- and C3-naphthobenzothiophenes (NBT2 and NBT3). These data imply that while the groups were initially similar (based on the relative NBT concentrations), the dispersant-mediated samples' PA2 and PA3 were more weathered (in reduced proportion) and thus had been removed more rapidly than in the samples without detectible dispersant indicators (non-dispersed). Additional PAH groups are plotted and statistically assessed (Tabesh et al., 2010) in the Supplemental Information (SI) (Figure S- 1 and Table S- 1). The overall conclusion is that more-soluble PAH show greater loss in the dispersant-treated groups. Less-soluble, higher-molecular-weight PAH (e.g., naphthobenzothiophenes) show little to no difference.

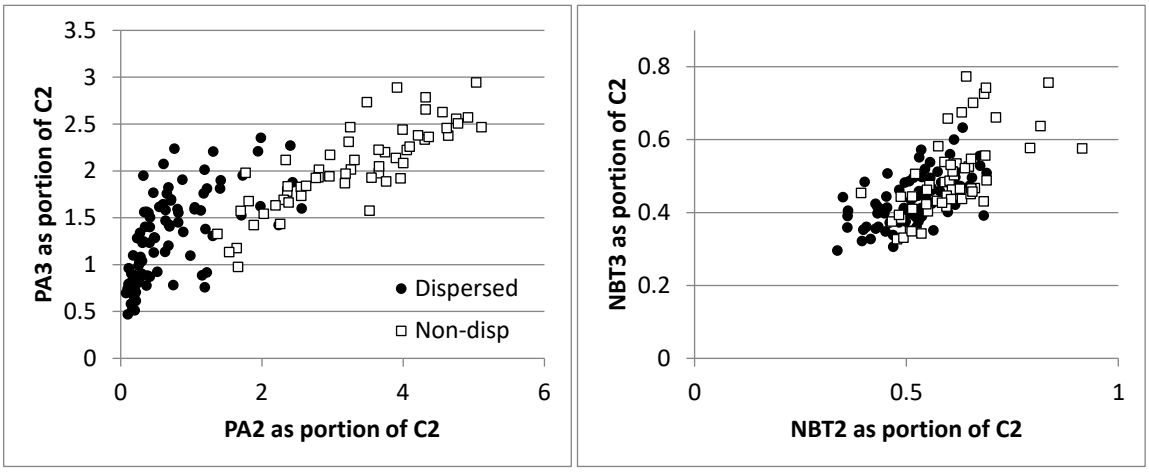

Figure 4. PAH distributions from dispersant-treated (dots) and untreated (boxes) water samples. All concentrations are normalized to the sample's C2-chrysene. Clustering of conservative NBT ratio components (right panel) suggests all samples were similar while phenanthrene groups (left panel) were discriminated by dispersant treatment. Samples are MC252-confirmed, particulate samples with no dissolved components. n = 133 dispersed, 71 non-dispersed.

One easily observed effect of accelerated weathering is seen in the classic forensic tool, the dibenzothiophene/phenanthrene (D/P) double-ratio plots (Douglas et al., 1996). With normal weathering, the alkylated-homologue pairs from each of these PAH groups have similar K_{OW} values and thus degrade at similar rates. The phenanthrenes/anthracenes, however, degrade slightly faster than the sulfur-containing dibenzothiophenes, likely through a combination of dissolution and differential microbial degradation. In plotting the C2-alkylated forms against the C3-alkylated forms, the weathering trend for non-dispersed oil is predictable and mostly linear (Figure 5). In contrast, dispersant-mediated samples tend to lose the C2-phenanthrenes quicker than the other three C2- and C3- components and

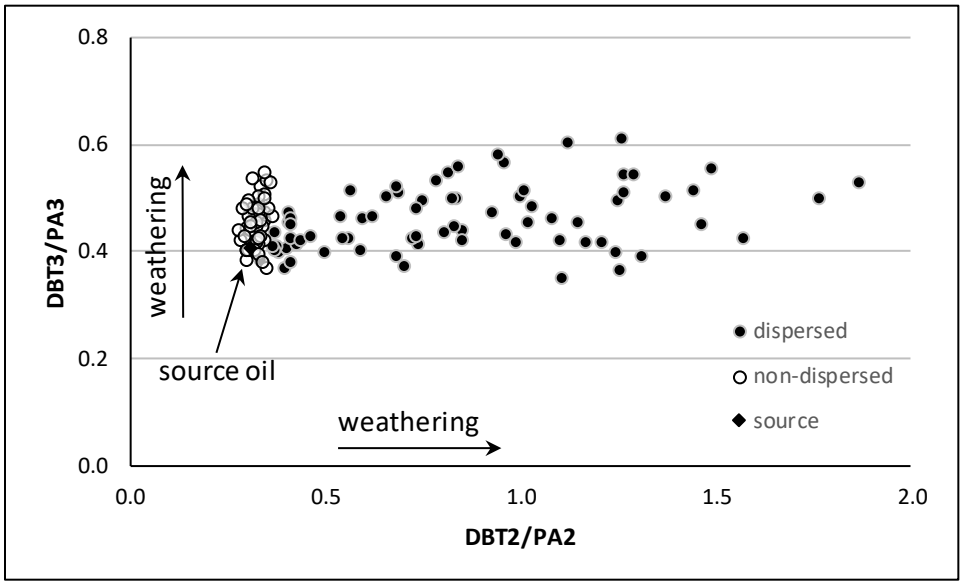

Figure 5. Comparison of dispersed versus non-dispersed DWH water samples in double-ratio weathering plot of C2- and C3-alkylated dibenzothiophenes (DBT) and phenanthrene/anthracenes (PA). Lateral spread in dispersant-mediated samples is attributed primarily to accelerated loss of C2-phenanthrenes. Points represent filters and whole waters with only particulate profiles (whole oil only, no dissolved components) from the DWH NRDA data set.

thus, create a unique "low path" trend laterally across the plot. The presented plotted data were meticulously screened to use only forensically-confirmed DWH NRDA field samples (water or filters) with particulate-phase profiles but without any dissolved-phase components (only 204 of the 493 samples assessed with particulate profiles; see Part 1 of this article series, Payne and Driskell, 2018). Including any of the variable, dissolved phase components in this analysis would confound the individual analyte concentrations. We postulate that the large scatter among dispersed samples (Figure 5) may be a stochastic effect from highly variable dispersant concentrations.

Also using the publicly available, online NRDA data, Spier et al. (2013) independently concluded that application of subsurface dispersants increased hydrocarbon concentrations at depth based on total hydrocarbon detects, but they did not provide any finer insights to the process. These results were further corroborated by laboratory tank tests demonstrating the dispersant's effectiveness in breaking up the oil droplets (Brandvik et al., 2013 and Johansen et al., 2013), but not the heretofore hypothesized, accelerated stripping of lower- and intermediate-molecular-weight PAH from the oil droplets into the dissolved phase (NRC 2005). Recent work summarizing simulations of hypothetical blowouts using multiple models concluded that, for the limited cases studied, applying chemical dispersants at the DWH wellhead would yield a 200-fold reduction on the interfacial tension between oil and water, thereby producing at least an order-of-magnitude reduction in droplet size (Socolofsky et al., 2015). As expected in these scenarios, the smaller droplets were predicted to degrade much faster than

the untreated, larger droplets due to the smaller droplet's higher surface-area-to-volume ratio and longer rise time. In high crossflow simulations with fate processes included, up to 95% of the released oil remained submerged within 14 days of release. These studies and analyses, plus other DWH field data (Spaulding et al., 2015), corroborate the findings presented here that the dispersants injected at depth actually worked. From our forensic assessments, NRDA samples taken in the deep plume and showing dispersant-modified profiles (showing enhanced dissolution) ranged out to 183 km SW of the wellhead (Payne and Driskell 2015a, 2016, 2018).

Microbial SHC Degradation

The data presented so far in this paper focus on early stage weathering where abiotic processes have dominated. A droplet's n-alkanes and isoprenoids making up the SHC are compounds that are normally preferentially degraded by microbes prior to any significant PAH losses (Bartha and Atlas, 1977). In these dispersant-treated profiles, they were mostly intact and looking remarkably fresh relative to the extent of PAH weathering. Except for dissolution losses of the slightly soluble C_9-C_{13} n-alkane components, there appears to be minimal microbial impact (lower SHC profiles in Figure 3 and Supplemental Information (SI) (Figure S- 2 and Figure S- 3). Thus, arises the question: do these data suggest that biotic processes (i.e., biodegradation) were truly inhibited or merely that the accelerated abiotic dissolution occurred on such a short time scale that microbial processes were not fully engaged when the samples were taken? While we are unable to resolve this question solely from uncontrolled NRDA field results, the following discussion provides insight relevant for oil-spill researchers, assessors and responders.

Oil biodegradation is a complex process involving both water-suspended (planktonic) microbial communities and those attaching to oil surfaces (sessile) (Brakstad et al., 2015; Kapellos et al., 2018). With particulate-phase oil, microbes work the surface of oil droplets in biofilm communities either by direct contact at the oil-water interface or through the aqueous medium at a microscale separation (Ward, 2010). During catabolism, extracellular enzymes (mostly mono- and dioxygenases in aerobic circumstances) break down and transport otherwise insoluble hydrocarbons across the cellular membrane (Gutierrez et al., 2013). Logically, breaking the oil into smaller droplets with chemical dispersants would increase the oil-water interface and thus, the space available for microbial attachment and growth plus increased diffusion from the increased surface area. And not surprisingly, several laboratory studies have shown that dispersants can increase biodegradation (Siron et al., 1995; Venosa and Holder, 2007; Prince et al., 2013; McFarlin et al., 2014; Brakstad et al., 2014). Brakstad et al. (2015) demonstrated biodegradation inversely correlated with droplet sizes in dispersion, i.e., faster biotransformation of the low-range and medium-range molecular-weight n-alkanes occurred in 10 µm versus 30 µm droplet-size dispersions. They concluded that the use of dispersants in seawater to generate small droplets would promote faster rates of biodegradation in otherwise similar environmental conditions. Chakraborty et al. (2012) reported that microbes enriched from the dispersed DWH plume were able to degrade oil better and could also readily degrade certain dispersant components.

However, in the DWH NRDA field data, the lack of significant SHC degradation in high-concentration, dispersant-mediated samples close to the wellhead does not support a simple droplet-size-driven

concept (SI, Figure S- 2). In previous studies with microbial consortia at 8° C, Corexit 9500 added to fresh or weathered oil had not shown any change in oil degradation (Lindstrom and Braddock, 2002). Other studies posited a diversity of explanations for inhibition. For example, an inhibitory effect may have arisen from soluble C_5-C_{10} alkane homologues (e.g., pentane, hexane, heptane, octane, nonane, and decane) (Bartha and Atlas 1977) and mono-cycloaliphatic compounds (e.g., cyclopentane, cyclohexane, and cycloheptane) (Leahy and Colwell, 1990) that were in high concentrations close to the wellhead early in the spill (Payne and Driskell, 2015a). Acting as solvents, they could easily disrupt biological reactions, extra-cellular products, or components (e.g., lipid membranes). Edwards, et al. (2011) suggested initial microbial degradation at depth may have been carbon rich but nutrient limited. Schedler et al. (2014) report high-pressure (depth) effects causing markedly diminished hydrocarbon-degradation rates in one microbial strain but not another. Prince et al. (2013) noted that highly concentrated dispersed-oil droplets, BTEX, or surfactants may initially inhibit microbial degradation of hydrocarbons until PAH and SHC are diluted to levels more suitable to their metabolic or extracellular exudates' functionality. Campo et al. (2013) and Brakstad et al. (2015) noted inhibited or delayed n-alkane degradation in oil/dispersant/microcosm studies at 5° C. Venosa (2013) suggested that the conceptual inhibition in this study's DWH data may have been due to the SHC fraction's impermeability due to a frozen, condensed, waxy, solid-phase state. Recent results from Rahsepar et al. (2016) strive to advance the understanding using monocultures in lab microcosms. Using fresh and weathered MC252 oil both with and without Corexit 9500, they found Corexit delayed initial growth and alkane degradation at typical application levels (DOR 1:20). They attribute the inhibitory effect to dispersant's release of BTEX from fresh crude oil as the effect was diminished either by inoculating with both alkane and BTEX degrading cultures or starting with weathered oil. These results are invocative of a possible delay mechanism but actually only describe effects in a simple lab system.

However, Makar and Rockne (2003) among others and single-species microcosm work by Bookstaver et al. (2015) suggests a different cause; the ionic nature of attached dispersant molecules may interfere with the effectiveness of natural microbial biosurfactants and thereby inhibit attaching and creating biofilms. This finding is understandable considering the complexity of micro-scale biochemical processes occurring as microbes transition from a planktonic state into attached biofilms (Sauer et al., 2007), for example, functional shifts in gene expression and proteonomics occur before, during, and after the biofilm transitions. Generically, for direct contact to be made between the hydrophobic surface of a non-dispersed oil droplet and a microbe's hydrophobic (lipid) membrane, biosurfactants mediate the process. The microbe's bioemulsifiers subsequently create the micelles to transfer the oil hydrocarbons to the awaiting mono- and dioxygenase enzymes, either extra-cellular or membrane-bound, to further process, transfer and eventually internally catabolize the oil (Chróst, 1990; Vetter et al., 1998). And the story becomes even more complex as biofilms are formed and different species are communicating and interacting competitively and syntrophically within a community (McGenity et al., 2012, Hazen et al., 2016). Shapiro (2007) attributes computational, cognitive, and evolutionary capabilities to microbes in recognition of their bioengineering complexity, communal communication, plasticity, and resilience. Thus, in regard to dispersants, it seems logical to presume that each microbial strain will have its individual response with some inhibited by and some promoted by the chemistry of a given dispersant (Overholt et al., 2016). Another case of inhibition may occur when dispersants are present in

concentrations above their critical micelle concentration (CMC); hydrocarbons completely partitioned in dispersant micelles simply may not be bioavailable (Bookstaver et al., 2015). From our data, considering the amphipathic polar nature of the Corexit dispersant and high levels reported within our reference series (Figure S- 2), the observed "inhibited" biodegradation of SHC might be expected.

Most recently, Brakstad et al. (2017) detailed biodegradation chemistry and microbial succession using a metagenomics approach on natural cultures in microcosms at various oil/dispersant concentrations. In their approach, they point out that once the oil is chemically dispersed, rapid dilution occurs in the water column. While trying to simulate natural conditions, they found essentially no effect from dispersants. In reality, natural processes are not easily simulated nor described by simple chemical or engineering models attempting to portray average tendencies. Biodegradation of a complex contaminant, such as oil, invokes a complex microbial community response. During the DWH event, early reports suggesting aliphatics were rapidly biodegraded (within a few weeks; Hazen et al., 2010), were later countered by further observations, modelling and negated by reanalysis of the data (Valentine et al., 2012; Bagby et al., 2016). Valentine et al. summarized that currents, mixing processes, and autoinoculation created a complex dynamic that would affect priming of native microbiota and subsequent biodegradation efficiencies. Bagby et al. interpreted DWH water and sediment data to suggest that biodegradation rates varied inversely with contamination loads and that biodegradation advanced more rapidly while the oil was suspended in the water column than after its deposition to the sea floor.

Despite contrasting findings from various studies, with additional time and distance from the wellhead, biodegradation of both dispersant-mediated and non-dispersant-mediated oil was comprehensive in depleting the oil in the plume (reviewed by Chakraborty et al., 2012, and Kimes et al., 2014). In benthic sediments, all but the longest-chain n-alkanes were eventually degraded, with the degree of degradation increasing with distance from the well (Stout and Payne, 2016), suggesting n-alkanes were gradually degraded in oil particles as they advected away from the well and prior to deposition.

These conclusions point to the functional utility of dispersants for reducing oil-droplet sizes and thus limiting oil rising to the surface and potentially being transported to shorelines. However, enhanced dissolution and retention at depth also suggests increased bioavailability of BTEX and certain PAH to benthic and pelagic organisms.

Summary

For the first time, dispersant indicators, measured in field-collected, particulate-phase oil samples from deep plume depth, documented the effect of wellhead dispersant injections. Dispersant application resulted in markedly enhanced abiotic dissolution of lower- and intermediate-molecular-weight PAH compared to non-dispersant-mediated oil. Unlike larger oil droplets buoyantly rising in the water column, once dissolved, these components (along with smaller, less buoyant droplets) would have moved within the plume and been subjected to further microbial degradation. From available data, we are unable to distinguish whether the relative delay noted in SHC biodegradation is truly attributable to inhibited aliphatic biodegradation (e.g., by micellization, lack of effective biosurfactants or biosurfactant

production, or crystallization of chilled aliphatics) or merely represents a short-elapsed-time view of high-concentration processes near the release point.

Elucidating the effects of dispersants on oil droplets at depth was a fortuitous finding. Without the opportune convergence of a clean ocean background, an entrained plume, and high dispersant and oil concentrations, it would have been difficult to recognize the purely dispersant-mediated effect. Relying solely on the PAH patterns, these samples would have been enigmatically classified as a mixture or an anomalous "other oil." Furthermore, the now revealed physical/chemical dynamics of accelerated PAH depletion (up through dibenzothiophenes) will certainly prompt further investigations into dispersant/oil interactions. From NRDA field data, samples with actual dispersant-modified profiles (i.e., not just containing dispersant indicators) comprised 192 of the 1,769 *Deepwater-Horizon*-matched water samples with the furthest in the plume, 183 km SW of the wellhead. An extant plume with dispersant indicators but no significant oil-relevant PAH ranged to 412 km from the wellhead (Payne and Driskell, 2015a, 2016, 2018).

Acknowledgment

This work is primarily based on water samples collected, analyzed and assessed as part of the DWH NRDA to which the authors served as technical contractors. The interpretations presented in this paper reflect the opinions of the authors and not necessarily those of NOAA or the DWH Trustees. We would especially like to thank NOAA and consultant colleagues on the Trustees Chemistry and Data Management Groups and our fellow forensic chemists at NewFields for the collaborative efforts. Additional thanks to Al Venosa and Joan Braddock for reviewing and validating the microbial concepts. And finally to Katz, Murphy and Gopalan for use of the incredibly insightful photos of the streaming, dispersed droplets.

References

Bartha, R. and R.M. Atlas. 1977. The microbiology of aquatic oil spills. In: D. Perlman (ed.), Advances in Applied Microbiology. Academic Press, pp. 225-266.

Bagby, S.C., C.M. Reddy, C. Aeppli, G.B. Fisher, and D.L. Valentine. 2016. Persistence and biodegradation of oil at the ocean floor following *Deepwater Horizon*. *Proc Natl Acad Sci* U S A. 2017 Jan 3;114(1):E9-E18. doi: 10.1073/pnas.1610110114. Epub 2016 Dec 19.

Bejarano, A.C., E. Levine, and A.J. Mearns. 2013 Effectiveness and potential ecological effects of offshore surface dispersant use during the *Deepwater Horizon* oil spill: a retrospective analysis of monitoring data. *Environ Monit Assess* 185:10281. doi:10.1007/s10661-013-3332-y

Bookstaver, M., A. Bose, and A. Tripathi. 2015. Interaction of *Alcanivorax borkumensi*s with a surfactant decorated oil–water interface. *Langmuir* 31 (21), 5875-5881. DOI: 10.1021/acs.langmuir.5b00688

British Petroleum (BP). 2014. Gulf Science Data Reference Oil Characterization Data. Website: http://gulfsciencedata.bp.com/, directory: Other; subdirectory: Dispersant Application; filename: DispersantApplication_OTH-02v01-01.xlsx and DispersantApplication_OTH-02v01-02.xlsx. Last modified January 24, 2014.

Brakstad, O.G., P.S. Daling, L.-G. Faksness, I.K. Almas, S.-H. Vang, S. Syslak and F. Leirvik. 2014. Depletion and biodegradation of the Macondo 252 oil in dispersions and emulsions generated in an oil-on-seawater mesocosm flume basin. *Mar. Pollut. Bull.* 84, 125–134.

Brakstad, O.G., T. Nordtug and M. Throne-Holst. 2015. Biodegradation of dispersed Macondo oil in seawater at low temperature and different oil droplet sizes. *Mar. Pollut. Bull.* 93: 144–152.

Brakstad, O.G., D. Ribicic, A. Winkler, R. Netzer. 2017. Biodegradation of dispersed oil in seawater is not inhibited by a commercial oil spill dispersant. *Mar Pollut Bull.* pii: S0025-326X(17)30876-7. doi: 10.1016/j.marpolbul.2017.10.030

Brandvik, P.J., Ø. Johansen, F. Leirvik, U. Farooq and P.S. Daling. 2013. Droplet breakup in subsurface oil releases – Part 1: Experimental study of droplet breakup and effectiveness of dispersant injection. *Mar. Pollut. Bull.* 73(1): 319-326.

Campo, P., A.D. Venosa, and M.T. Suidan. 2013. Biodegradability of Corexit 9500 and dispersed South Louisiana crude oil at 5 and 25^{o} C. *Environ. Sci. Technol.* 47: 1960-1967.

Chakraborty R., S.E. Borglin, E.A. Dubinsky, G.L. Andersen and T.C. Hazen. 2012. Microbial response to the MC-252 oil and Corexit 9500 in the Gulf of Mexico. *Front. Microbio.***3**:357. doi: 10.3389/fmicb.2012.00357

Chróst, R. 1990. Microbial ectoenzymes in aquatic environments, p 47–78. *In J.* Overbeck and R. Chróst (eds), Aquatic microbial ecology. Springer,New York, NY.

Coastal Response Research Center (CRRC). 2010. *Deepwater Horizon* Dispersant Use Meeting Report. University of New Hampshire, Durham, NH, 21 pp and appendices.

Davis, C. S. and N. C. Loomis. 2014. *Deepwater Horizon* Oil Spill (DWHOS) Water Column Technical Working Group, Image data processing plan: holocam description of data processing methods used to determine oil droplet size distributions from in situ holographic imaging during June 2010 on cruise *M/V Jack Fitz* 3. Woods Hole Oceanographic Institution and MIT/WHOI Joint Program in Oceanography. 15 pages + Appendices.

Douglas, G.S., A.E. Bence, R.C. Prince, S.J. McMillen, and E.L. Butler. 1996. Environmental stability of selected petroleum hydrocarbon source and weathering ratios. *Environ. Sci. Technol.* 30(7): 2332-2339.

Edwards, B.R., C.M. Reddy, R. Camilli, C.A. Carmichael, K. Longnecker, and B.A.S. Van Mooy. 2011. Rapid microbial respiration of oil from the *Deepwater Horizon* spill in offshore surface waters of the Gulf of Mexico. *Environ. Res. Lett*. 6: 035301.

French-McCay, D.P, K. Jayko, Z. Li, M. Horn, Y. Kim, T. Isaji, D. Crowley, M. Spaulding, S. Zamorski, J. Fontenault, R. Shmookler, and J.J. Rowe. 2015. Technical Reports for *Deepwater Horizon* Water Column Injury Assessment – WC_TR.14: Modeling oil fate and exposure concentrations in the deepwater plume and rising oil resulting from the *Deepwater Horizon* oil spill. RPS ASA, South Kingstown, RI, USA, August 2015.

French-McCay, D., M. Horn, Z. Li, K. Jayko, M. Spaulding, D. Crowley, D. Mendelsohn. 2018. Modeling distribution, fate, and concentrations of *Deepwater Horizon* oil in subsurface waters of the Gulf of Mexico. Oil Spill Environmental Forensics – Case Studies, S.A. Stout and Z. Wang (eds.), Elsevier/Academic Press. Pp. 683-735.

Gopalan, B. and J. Katz. 2010. Turbulent shearing of crude oil mixed with dispersants generates long microthreads and microdroplets. *PRL* 104, 054501, 4 pp.

Gray, J.L., L.K. Kanagy, E.T. Furlong, J.W. McCoy, and C.J. Kanagy. 2011. Determination of the anionic surfactant di(ethylhexyl)sodium sulfosuccinate in water samples collected from Gulf of Mexico coastal waters before and after landfall of oil from the *Deepwater Horizon* oil spill, May to October, 2010. U.S. Geological Survey Open-File Report 2010-1318, 15 p <http://www.pubs.usgs.gov/of/2010/1318/>

Gray, J.L., L.K. Kanagy, E.T. Furlong, C.J. Kanagy, J.W. McCoy, A. Mason, and G. Lauenstein. 2014. Presence of the Corexit component dioctyl sodium sulfosuccinate in Gulf of Mexico waters after the 2010 *Deepwater Horizon* oil spill. *Chemosphere* 95: 124-130.

Gutierrez, T., D. Berry, T. Yang, S. Mishamandani, L. McKay, A. Teske, and M.D. Aitken. 2013. Role of bacterial exopolysaccharides (EPS) in the fate of the oil released during the *Deepwater Horizon* oil spill. *PLOS ONE* 8(6): e67717

Hazen, T.C., E.A. Dubinsky, T.Z. DeSantis, G.L. Andersen, Y.M. Piceno, N. Singh, J.R. Jansson, A. Probst, S.E. Borglin, J.L. Fortney, W.T. Stringfellow, M. Bill, M.S. Conrad, L.M. Tom, K.L. Chavarria, T.R. Alusi, R. Lamendella, D.C. Joyner, C. Spier, M. Auer, M.L. Zemla, R. Chakraborty, E.L. Sonnenthal, P. D'haeseleer, H.-Y.N. Holman, S. Osman, Z. Lu, J.D. Van Nostrand, Y. Deng, J. Zhou, and O.U. Mason. 2010. Deep-sea oil plume enriches indigenous oil-degrading bacteria. *Science* 330, 204–208. doi: 10.1126/science.119597

Hazen, T.C., R.C. Prince, and N. Mahmoudi. 2016. Marine Oil Bioremediation. *Environ. Sci. Technol*. 50:2121-2129. DOI: 10.1021/acs.est.5b03333.

Johansen, Ø, P.J. Brandvik and U. Farooq. 2013. Droplet breakup in subsea oil releases – Part 2: Predictions of droplet size distributions with and without injection of chemical dispersants. *Mar. Pollut. Bull.*, 73(1): 327-335.

Kapellos, G.E., C.A. Paraskeva, N. Kalogerakis, P.S. Doyle. 2018. Theoretical insight into the biodegradation of solitary oil microdroplets moving through a water column. *Bioengineering* (Basel) 5(1). pii: E15. doi: 10.3390/bioengineering5010015

Katz, J. 2009. Measurements and modeling of size distributions, settling, and dispersions (turbulent diffusion) rates. Final Report prepared for the Coastal Response Research Center. August 2009. 31 pp.

Katz, J., D.W. Murphy and D. Morra. 2013. Large scale behavior and droplet size distributions in crude oil jets and plumes. American Physical Society. 66th Annual Meeting of the Division of Fluid Dynamics, Pittsburgh, PA. November 24-26, 2013.

Kimes, N.E., A.V. Callaghan, J.M. Suflita and P.J. Morris. 2014. Microbial transformation of the *Deepwater Horizon* oil spill—past, present, and future perspectives. *Front. Microbiol.* 5:603. doi:10.3389/fmicb.2014.00603

Kujawinski, E.B., M.C.K. Soule, D.L. Valentine, A.K. Boysen, K. Longnecker, and M.C. Redmond. 2011. Fate of dispersants associated with the *Deepwater Horizon* oil spill. *Environ. Sci. Technol.* 45(5): 1298-1306.

Leahy, J.G. and R.R. Colwell. 1990. Microbial degradation of hydrocarbons in the environment. *Microbiological Reviews* 54(3), 305-315.

Li, C., A. Hosler, and J. Katz. 2013. Breakup of an oil slick mixed with dispersant by breaking wave. American Physical Society. 66th Annual Meeting of the Division of Fluid Dynamics, Pittsburgh, PA. November 24-26, 2013.

Li, Z., A. Bird, J. Payne, N. Vinhateiro, Y. Kim, C. Davis and N. Loomis. 2015. Draft physical-chemical technical reports for *Deepwater Horizon* Water Column Trustees: Volume III, oil particle data from the *Deepwater Horizon* oil spill.

Li, Z., M. L. Spaulding, D. French McCay, D. Crowley, and J.R. Payne. 2016. Development of a unified oil droplet size distribution model with application to surface breaking waves and subsea blowout releases considering dispersant effects. *Mar. Pollut. Bull.* 114 (1): 247–257.

Lindstrom, J.E., and J.F. Braddock. 2002. Biodegradation of petroleum hydrocarbons at low temperature in the presence of the dispersant Corexit 9500. *Mar. Pollut. Bull.* 44, 739–747.

Makkar, R.S. and K.J. Rockne. 2003. Comparison of synthetic surfactants and biosurfactants in enhancing biodegradation of polycyclic aromatic hydrocarbons. *Environ Toxicol Chem* 2003; 22:2280-2292.

McFarlin, K.M., R.C., Prince, R. Perkins and M.B. Leigh. 2014. Biodegradation of dispersed oil in Arctic seawater at – 1_C. *PLOS ONE* 9, e84297.

McGenity, T.J., B.D. Folwell, B.A. McKew, G.O. Sanni. 2012. Marine crude-oil biodegradation: a central role for interspecies interactions. *Aquat. Biosyst*. 2012, 8, 10

Murphy, D.W., C. Li, V. dAlbignac, D. Morra and J. Katz. 2015. Splash behaviour and oily marine aerosol production by raindrops impacting oil slicks. *J. Fluid Mech.*, 780, 536–577.

Nagamine, S.I. 2014. The effects of chemical dispersants on buoyant oil droplets. Master's Thesis, University of Hawaii at Manoa, May 2014. 122 p.

National Research Council (NRC). 2005. Oil Spill Dispersants: Efficacy and Effects. National Academy Press, Washington D.C., 377 pp.

NOAA. 2014. Analytical quality assurance plan, Mississippi Canyon 252 (*Deepwater Horizon*) natural resource damage assessment, Version 4.0. May 30, 2014.

Overholt, W.A., K.P. Marks, I.C. Romero, D.J. Hollander, T.W. Snell, J.E. Kostka. 2016. Hydrocarbon-degrading bacteria exhibit a species-specific response to dispersed oil while moderating ecotoxicity. *Appl. Env. Microbiol* 82:518 –527. doi:10.1128/AEM.02379-15

Payne, J.R., T.J. Reilly, and D.P. French. 1999. Fabrication of a portable large-volume water sampling system to support oil spill NRDA efforts. *Proceedings of the 1999 Oil Spill Conference*, American Petroleum Institute, Washington, D.C., 1179-1184.

Payne, J.R. and C.J. Beegle-Krause. 2011. Physical transport and chemical behavior of dispersed oil. White paper commissioned for the CRRC Workshop: The Future of Dispersant Use in Spill Response. September 20-22, 2011. NOAA Disaster Response Center, Mobile, Alabama. Available at: http://www.crrc.unh.edu/workshops/dispersant_future_11/Dispersant_Initiative_FINALREPORT.pdf)

Payne, J.R. and W.B. Driskell. 2015a. 2010 DWH offshore water column samples—Forensic assessments and oil exposures. PECI Technical Report to the Trustees in support of the PDARP (www.doi.gov/deepwaterhorizon/admin record, DWH-AR0039118, 37 pp.).

Payne, J.R. and W.B. Driskell. 2015b. *Deepwater Horizon* oil spill NRDA offshore adaptive sampling strategies and field observations. PECI Technical Report to the Trustees in support of the PDARP. (www.doi.gov/deepwaterhorizon/admin record, DWH-AR0023786, 75 pp.).

Payne, J.R. and W.B. Driskell. 2015c. Forensic fingerprinting methods and classification of DWH offshore water samples. PECI Technical Report to the Trustees in support of the PDARP. (www.doi.gov/deepwaterhorizon/admin record, DWH-AR0039170, 31 pp.).

Payne, J.R. and W.B. Driskell. 2015d. Dispersant effects on waterborne oil profiles and behavior during the *Deepwater Horizon* Oil Spill. U.S. Dept. of Interior, *Deepwater Horizon* Response & Restoration, Admin. Record, *www.doi.gov/deepwaterhorizon/adminrecord*. DWH-AR0039201, 22 p. DWH NRDA Chemistry Technical Working Group Report, August 30, 2015.

Payne, J.R. and W.B. Driskell. 2016. Water column sampling for forensics. In Standard Handbook Oil Spill Environmental Forensics – Fingerprinting and Source Identification (2nd Edition), S. Stout and Z. Wang (eds.) Elsevier/Academic Press, 2016: 983-1014.

Payne, J.R. and W.B. Driskell. 2018. Macondo oil in northern Gulf of Mexico waters – Part 1: Assessments and forensic methods for *Deepwater Horizon* offshore water samples. *Mar. Pollut. Bull*. (submitted).

Prince, R.C., K.M. McFarlin, J.D. Butler, E.J. Febbo, F.C.Y. Wang and T.J. Nedwed. 2013. The primary biodegradation of dispersed crude oil in the sea, *Chemosphere*, 90(2): 521-526.

Rahsepar, S., Smit, M.P., Murk, A.J., Rijnaarts, H.H., Langenhoff, A.A., 2016. Chemical dispersants: oil biodegradation friend or foe? Mar. Pollut. Bull. 108, 113‑119.

Ryerson, T.B., K.C. Aikin, W.M. Angevine, E.L. Atlas, D.R. Blake, C.A. Brock, F.C. Fehsenfeld, R.-S. Gao, J.A. de Gouw, D.W. Fahey, J.S. Holloway, D.A. Lack, R.A. Lueb, S. Meinardi, A.M. Middlebrook, D.M. Murphy, J.A. Neuman, J.B. Nowak, D.D. Parrish, J. Peischl, A.E. Perring, I.B. Pollack, A.R. Ravishankara, J.M.

Roberts, J.P. Schwarz, J.R. Spackman, H. Stark, C. Warneke and L.A. Watts. 2011. Atmospheric emissions from the *Deepwater Horizon* spill constrain air/water partitioning, hydrocarbon fate, and leak rate, *Geophys. Res. Lett.*, 38, L07803, doi:10.1029/2011GL046726.

Sauer, K., A.H. Rickard, and D.G. Davies. 2007. Biofilms and Biocomplexity. *Microbe* 2:7, 347-353.

Schedler, M., R. Hiessl, A.G. Valladares Juárez, G. Gust and R. Müller. 2014. Effect of high pressure on hydrocarbon-degrading bacteria. *AMB Express*. 4:77. doi: 10.1186/s13568-014-0077-0. eCollection 2014.

Shapiro, J.A. 2007. Bacteria are small but not stupid: cognition, natural genetic engineering and socio-bacteriology. *Studies in History and Philosophy of Biological and Biomedical Sciences* 38:4 2007 Dec pg 807-819.

Siron, R., E. Pelletier and C. Brochu. 1995. Environmental factors influencing the biodegradation of petroleum hydrocarbons in cold seawater. *Arch. Environ. Contam. Toxicol.* 28, 406–416.

Socolofsky, S.A., E.E. Adams and C.R. Sherwood. 2011. Formation dynamics of subsurface hydrocarbon intrusions following the *Deepwater Horizon* blowout. *Geophys. Res. Lett.* 38: L09602.

Socolofsky, S.A., E.E. Adams, M.C. Boufadel, Z.M. Aman, Ø. Johansen, W.J. Konkel, D. Lindo, M.N. Madsen, E.W. North, C.B. Paris, D. Rasmussen, M. Reed, P. Rønningen, L.H. Sim, T. Uhrenholdt, K.G. Anderson, C. Cooper and T.J. Nedwed. 2015. Intercomparison of oil spill prediction models for accidental blowout scenarios with and without subsea chemical dispersant injection. *Mar. Pollut. Bull.* 96(1-2), 110-126. dx.doi.org/10.1016/j.marpolbul.2015.05.039.

Spaulding, M.S., D. Mendelsohn, D. Crowley, Z. Li and A. Bird. 2015. Technical Reports for *Deepwater Horizon* Water Column Injury Assessment—WC_TR 13. Application of OILMAP DEEP to the *Deepwater Horizon* Blowout. RPS ASA, 55 Village Square Drive, South Kingstown, RI 02879. August 2015.

Spier, C., W.T. Stringfellow, T.C. Hazen and M. Conrad. 2013. Distribution of hydrocarbons released during the 2010 MC252 oil spill in deep offshore waters. *Env. Poll*. 173: 224-230.

Stout, S.A. 2015. Review of dispersants used in response to the *Deepwater Horizon* oil spill. NewFields Technical Report TR02 to the Trustees in support of the PDARP.

Stout, S.A. and J.R. Payne. 2016. Macondo Oil in deep-sea sediments: Part 1 Sub-sea weathering of oil deposited on the seafloor. *Mar. Pollut. Bull.* 111: 365-380.

Tabesh, H., S. Ayatollahi, and M. Towhidi. 2010. A simple powerful bivariate test for two sample location problems in experimental and observational studies. *Theor Biol Med Model*. 2010: 7-13; doi: 10.1186/1742-4682-7-13

Valentine, D.L., I. Mezic, S. Macesic, N. Crnjarc-Zic, S. Ivic, P.J. Hogan, V.A. Fonoberov, and S. Loire. 2012. Dynamic autoinoculation and the microbial ecology of a deepwater hydrocarbon irruption. *PNAS* 1 108820 109.

Venosa, A.D. 2013. Biodegradation of DOSS and dispersed South Louisiana crude oil at two temperatures. Presented at the Gulf of Mexico Oil Spill & Ecosystem Science Conference. January 21-23, 2013. New Orleans, LA.

Venosa, A.D. and E.L. Holder. 2007. Biodegradability of dispersed crude oil at two different temperatures. *Mar. Pollut. Bull.* 54, 545–553.

Vetter, Y.A., J.W. Deming, P.A. Jumars, and B.B. Krieger-Brockett. 1998. A predictive model of bacterial foraging by means of freely released extracellular enzymes. *Microb. Ecol.*, 36, 75–92.

Ward, O.P. 2010. Microbial biosurfactants and biodegradation. In: Sen R, editor. Biosurfactants. Advances in experimental medicine and biology. Vol. 672. New York (NY): Springer Science+Business Media; 2010. p. 65–74.

White, H.K., S.L. Lyons, S.J. Harrison, D.M. Findley, Y. Liu, and E.B. Kujawinski. 2014. Long-term persistence of dispersants following the *Deepwater Horizon* oil spill. *Environ. Sci. Technol. Lett.* 1: 295-299.

Supplemental Information for

Macondo oil in northern Gulf of Mexico waters – Part 2: Dispersant-accelerated PAH dissolution in the *Deepwater Horizon* plume

William B. Driskell [a] and James R. Payne [b]

[a] 6536 20th Ave NE, Seattle, WA 98115
bdriskell@comcast.net

[b] Payne Environmental Consultants, Inc., 1651 Linda Sue Ln, Encinitas, CA 92024
jrpayne@sbcglobal.net

Dispersant-accelerated PAH-loss effect

The accelerated PAH-loss effect is demonstrated by comparing the individual PAH-analyte-ratio cluster dynamics from dispersant-mediated versus non-dispersed field samples (Figure S- 1). The PAH values are first normalized by each sample's conservative, alkylated C2-chrysene to effectively transform concentration values into relative weathering whereby movement towards the plot origin suggests dissolution loss of the less-alkylated component. Then, behavior of the treated and untreated (groups) of analyte pairs is appraised by overlaying the normalized values as bivariate scatterplots to highlight any differences in weathering rate patterns. For example, in normal dissolution weathering, C2-phenanthrene dissolves faster than C3-phenanthrene. If dispersants had no effect, there would be no significant difference between the two treatments; the group distributions would overlay each other. There are, however, strong visible differences (shift in group patterns) between the two treatments. For example, the group disparities for the C2- versus C3-phenanthrenes (PA2-PA3 plots in middle second row) imply two effects. First, the dispersant-treated samples' C2-phenanthrenes were weathering much faster than the non-dispersed samples causing a left shift in the dispersed pattern. Second, C3-phenanthrene was also degrading faster in the dispersed samples, resulting in a low-value sample cluster (samples aggregating nearer the plot origin). In contrast, the non-dispersed samples appear more evenly distributed across a range of higher values (less-weathered droplets). Moreover, looking at the samples' less-soluble naphthobenzothiophenes (NBT in bottom row), the treatment groups for the various alkylated isomers appear more tightly clustered and in overlapping patterns, suggesting both that the distribution of PAH values between the two groups was initially similar and, as expected, very little weathering occurred in either.

Statistically, 9 of the 14 treatment/PAH pairs showed significant differences in bivariate location of the two groups (Table S- 1) using a nonparametric Mann-Whitney U test per Tabesh et al. (2010). With the accelerated dissolution effect expected to decrease with increasing alkylation and molecular weight, the effect trends through the analyte groups as expected. The only anomaly is the FP2 vs FP3 data (fourth row), not unexpectedly, being strongly non-significant (p= 0.24) while FP3 vs FP4 data, also expected to show no differences, showed significant differences in the *opposite direction* (non-dispersed more weathered than dispersed, p=0.004). From just these data, this anomaly is inexplicable but is likely due

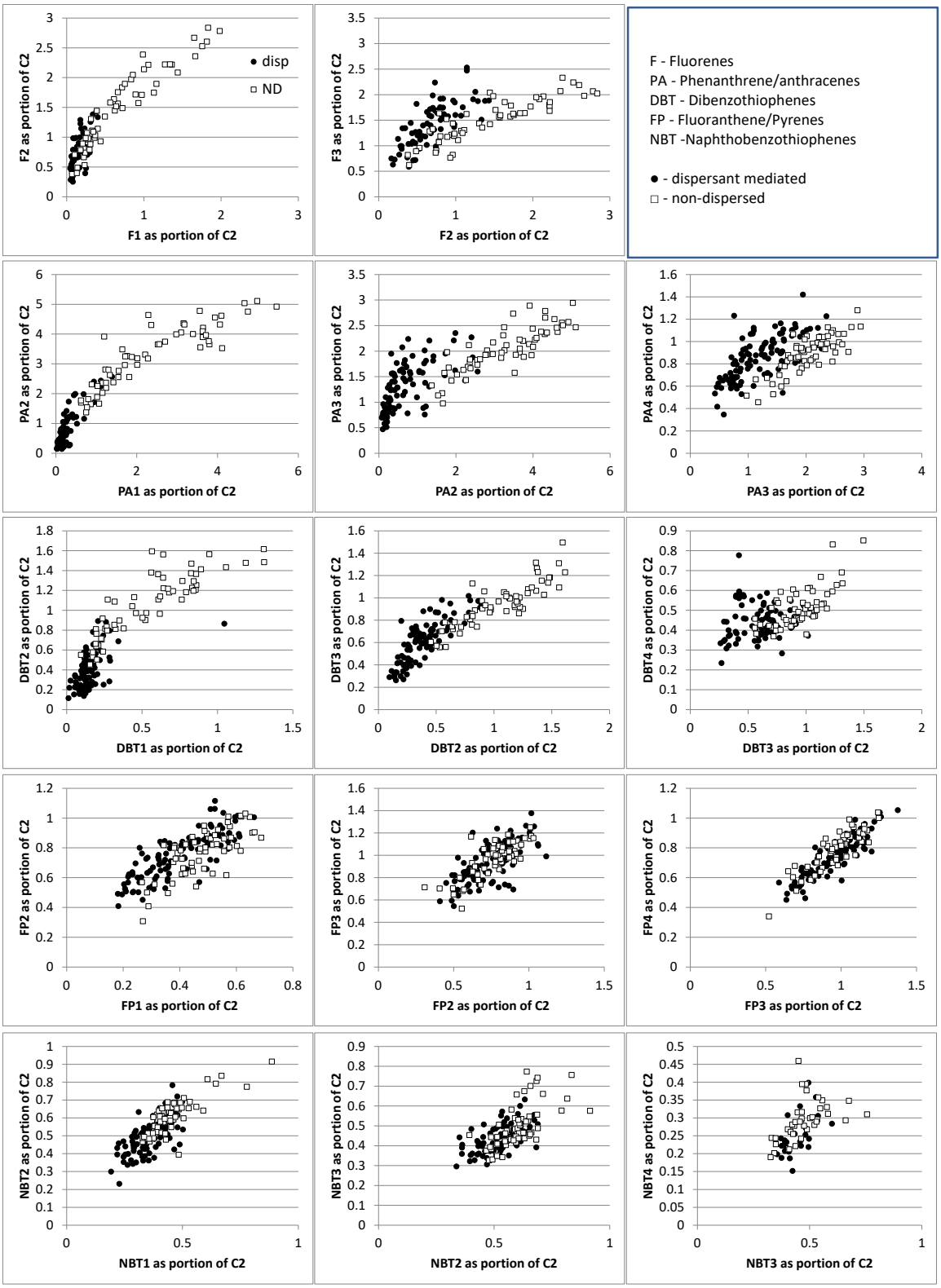

Figure S- 1. PAH distributions from dispersant-treated (dots) and untreated (boxes) water samples. All concentrations are normalized to the sample's C2-chrysene. Samples are MC252 matched particulate samples with no dissolved components. n = 133 dispersed, 71 non-dispersed.

Table S- 1. Statistical significance of differences in treatments in Figure S- 1 using Mann-Whitney U test for bivariate data; one-tailed, alpha = 0.05. Only 3 digits of p-value are presented.

parameter	p-value	signif	parameter	p-value	signif	parameter	p-value	signif
F1 vs F2	0.000	yes	F2 vs F3	0.000	yes	na		
PA1 vs PA2	0.000	yes	PA2 vs PA3	0.000	yes	PA3 vs PA4	0.000	yes
DBT1 vs DBT2	0.000	yes	DBT2 vs DBT3	0.000	yes	DBT3 vs DBT4	0.000	yes
FP1 vs FP2	0.001	yes	FP2 vs FP3	0.240	no	FP3 vs FP4	0.004	yes
NBT1 vs NBT2	0.094	no	NBT2 vs NBT3	0.314	no	NBT3 vs NBT4	0.290	no

to inherent lab quantification errors whereby the near- or below-reporting-limit homologues at the low end of the calibration curve can be overestimated for the summed abundance of 30-40 isomer peaks in the GC/MS chromatogram (note enhanced FP3 and FP4 reported in reference series, Figure S- 2). As discussed, the general accelerated-weathering trend is likely an enhanced dissolution effect as dispersants successively create smaller and smaller oil droplets. No attempt was made to adjust for the amount of dispersant relative to TPAH.

The evidence for only limited or delayed microbial degradation of the n-alkanes in the dispersant-mediated reference series is shown by persistent SHC patterns in the dispersed reference series (Figure S- 2) and by the minor reductions in the n-C_{17}/pristane and n-C_{18}/phytane ratios (Figure S- 3) that traditionally are used to track microbial processes (Bartha and Atlas, 1977). With sufficient time and distance from the wellhead, eventually all SHC were lost.

As a technical note, one reviewer has suggested using a higher-alkylated chrysene (C-3 or C-4) for standardizing the sample values. While correct on the basis that these would be less soluble and thus more recalcitrant than the C-2 chrysene used here, in practice, there is more lab error in quantifying the 30-40 isomer peaks most often in lower abundance on the GC/MS chromatogram than just the few generally higher peaks of C-2 chrysene. Similar logic applies to standardizing PAHs to C-2 napthobenzo thiophene, often used as our preferred conserved PAH, but here it became one of the comparison analytes. Standardizing using the triterpane biomarker, hopane, was also suggested as it is generally considered to be the gold standard for forensic evaluations; however, not all early DWH NRDA samples were analyzed for biomarkers.

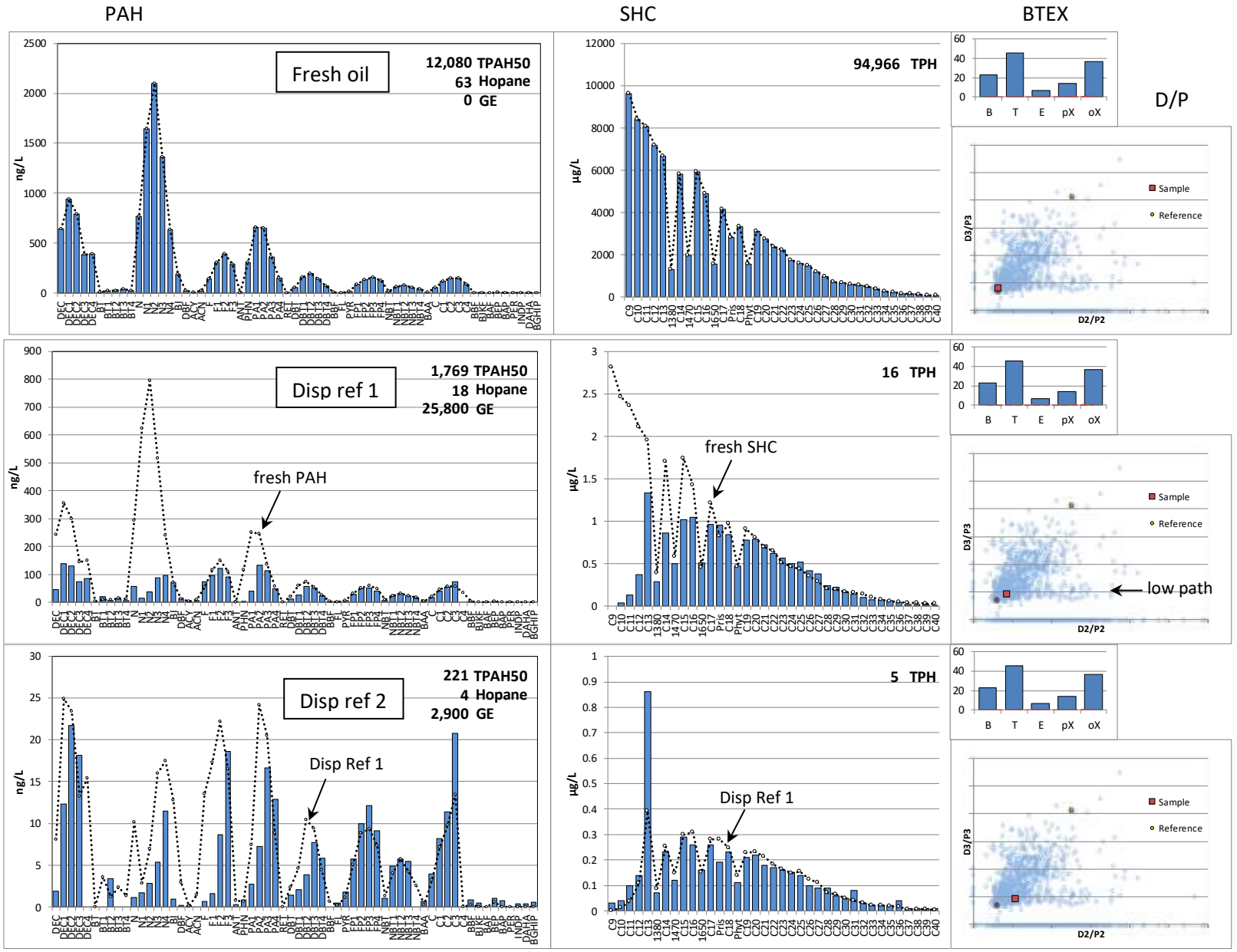
PAH
SHC
BTEX
Fresh oil
12,080 TPAH50
63 Hopane
0 GE
94,966 TPH
D/P
Disp ref 1
1,769 TPAH50
18 Hopane
25,800 GE
fresh PAH
16 TPH
fresh SHC
low path
Disp ref 2
221 TPAH50
4 Hopane
2,900 GE
Disp Ref 1
5 TPH
Disp Ref 1
Sample
Reference
D3/P3
D2/P2
B
T
E
pX
oX
µg/L

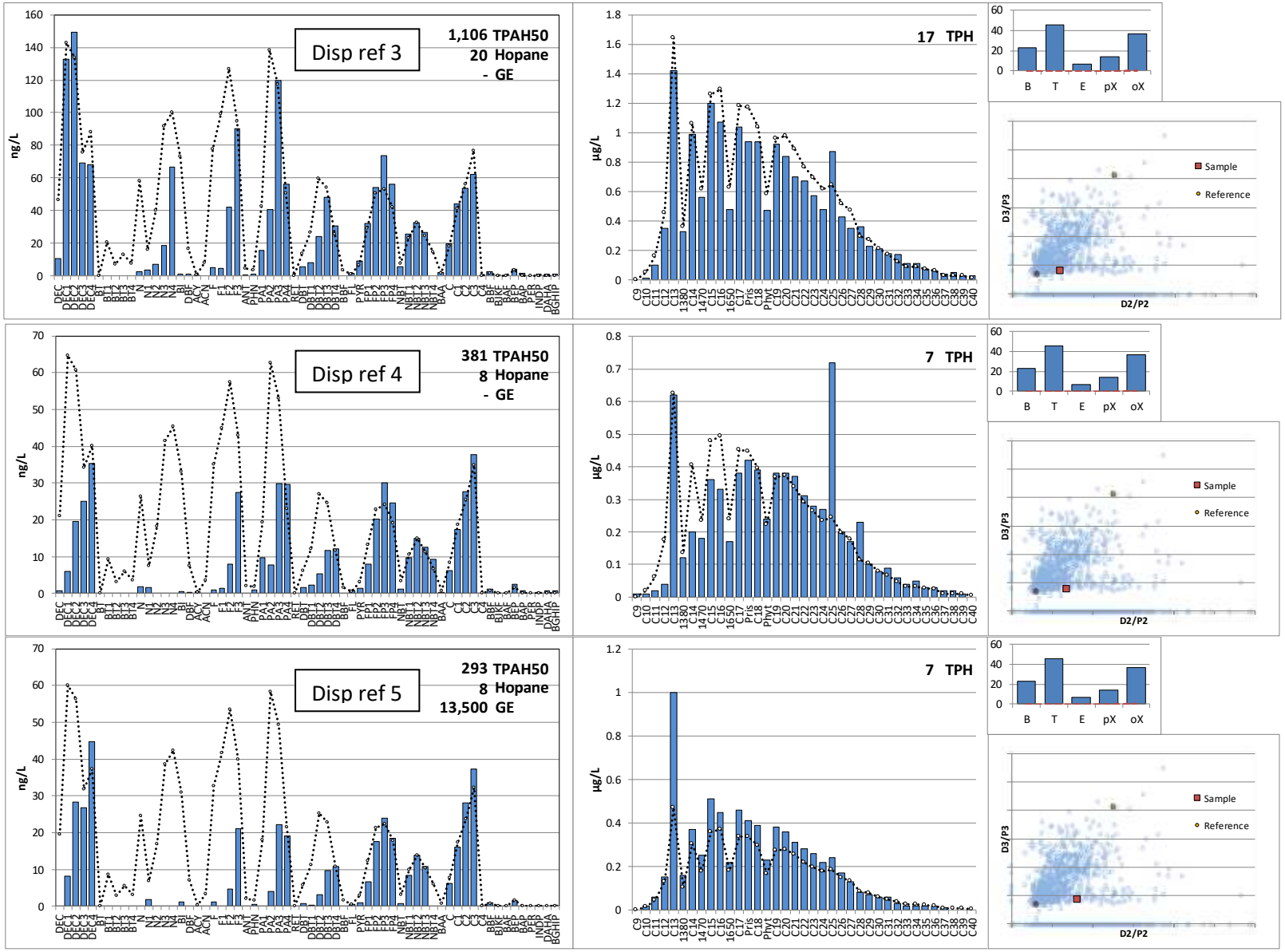
Disp ref 3
1,106 TPAH50
20 Hopane
- GE
17 TPH
Disp ref 4
381 TPAH50
8 Hopane
- GE
7 TPH
Disp ref 5
293 TPAH50
8 Hopane
13,500 GE
7 TPH
ng/L
µg/L
B T E pX oX
Sample
Reference
D3/P3
D2/P2

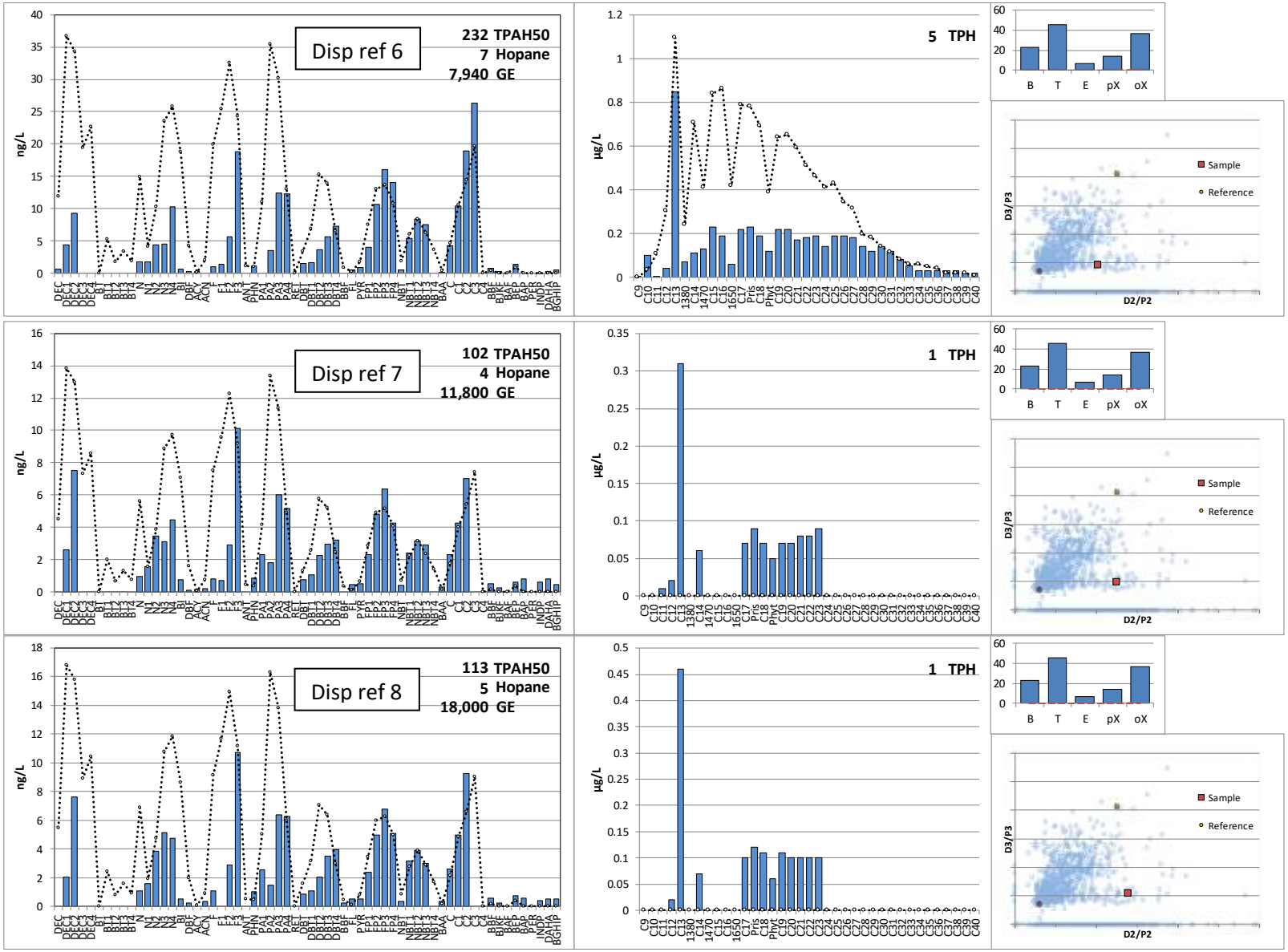
Disp ref 6
232 TPAH50
7 Hopane
7,940 GE
ng/L
5 TPH
µg/L
B T E pX oX
Sample
Reference
D3/P3
D2/P2
Disp ref 7
102 TPAH50
4 Hopane
11,800 GE
1 TPH
Disp ref 8
113 TPAH50
5 Hopane
18,000 GE

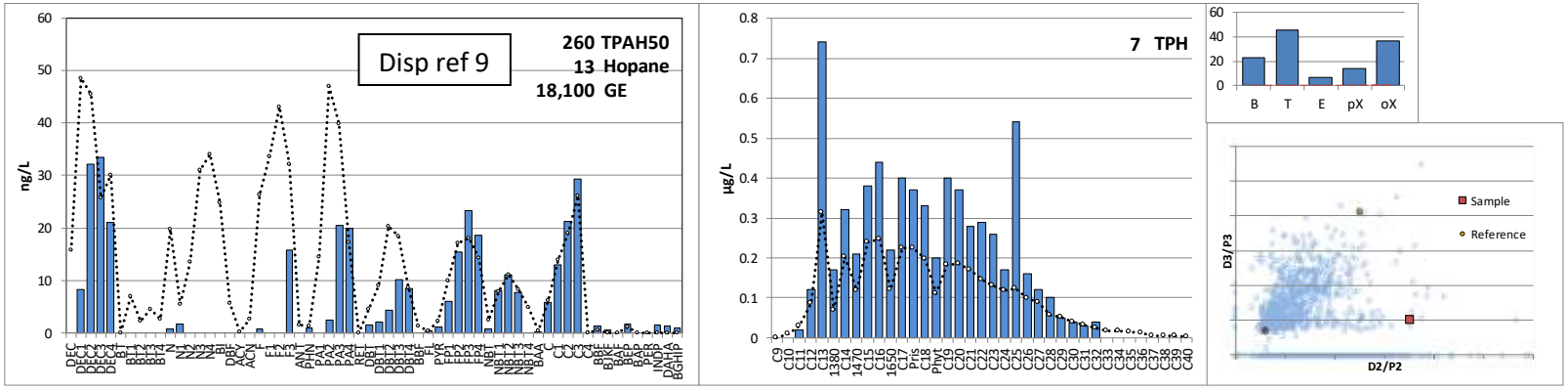

Figure S- 2. Reference series of 9 dispersant-mediated samples beginning with fresh oil (non-dispersed). Dotted line overlay in PAH plots series (left) is initially fresh oil and then dispersed reference 1 scaled to NBT2. GE concentrations (when measured) are given below hopane in the PAH plots. Center plots of SHC are similarly scaled to n-C_{26} (C_{25} when present, is a laboratory artifact). BTEX data and D/P double ratio plots are shown on right. Red square in D/P plots shows low path progression.

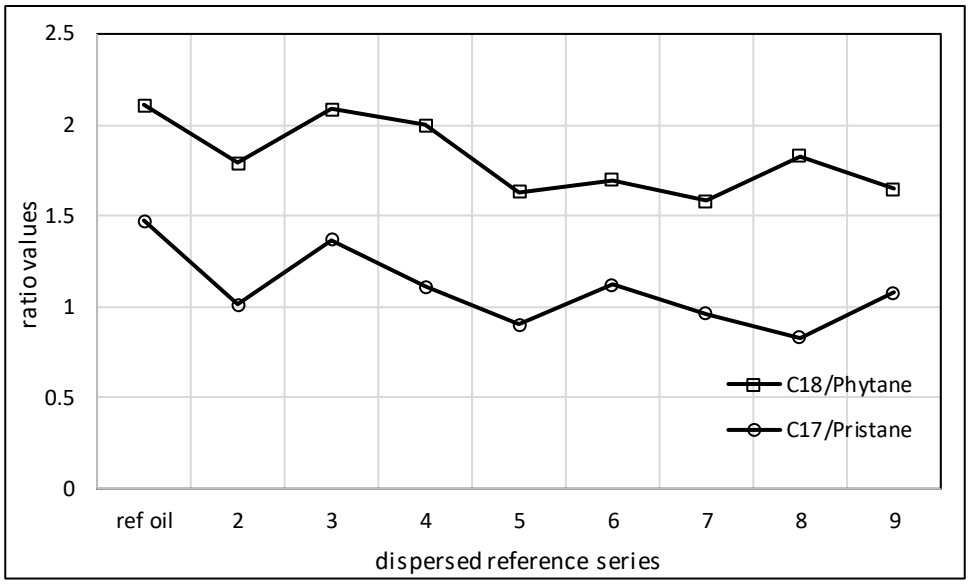

Figure S- 3. Biodegradation indicator ratios from dispersed reference samples (Figure S- 2) showing unusually slight SHC degradation throughout the series.